A Computational Study of Supersonic Combustion Relevant to Air–Breathing Engines

Christer Fureby, Ekaterina Fedina, and Jon Tegnér

1 Introduction and Background

The development of high–speed flight and space access vehicles requires the solution of many technical challenges associated with the comparatively small net thrust at supersonic or hypersonic flight speeds. One of the more essential issues is the design of an air–breathing propulsion system capable of operating over the wide range of Mach (Ma) numbers, desired to facilitate the advancement of high–speed flight and space access vehicles. At flight speeds above Ma≈3 turbofan engines fall short since the compressed air through the engine reaches such temperatures that the compressor stage fan blades begin to fail. Instead ramjet engines, in which the profile of the air intake guarantees that the supersonic approach flow is decelerated to a subsonic flow through the combustor, where fuel is injected prior to mixing, self-ignition and combustion, may be used. However, beyond Ma≈5 extreme temperatures and pressure losses occur when decelerating the supersonic airflow to subsonic conditions, making the ramjet unpractical at higher flight speeds. At flight speeds beyond Ma≈5, supersonic combustion ramjets, or scramjets, in which the flow trough the inlet and combustor remain supersonic may be used. Achieving high combustion efficiency under such conditions, with residence time on the order of 1 ms, places extreme demands on the inlet, combustor, fuel–injector as well as on the nozzle design, [1]. The mixing of fuel and air, the self–ignition and the flame stabilization are thus critical processes.

The prohibitive cost of flight–testing, difficulty in reproducing realistic flight conditions in ground facilities, the difficulties in measuring reacting flow quantities at supersonic speeds and the complexity of the aerothermodynamics involved make the use of Computational Fluid Dynamics (CFD) attractive for the analysis and design of high–speed flight vehicles. Conventional Reynolds Averaged Navier Stokes (RANS) models, [2], often provide no more than guidelines to the design

Christer Fureby · Ekaterina Fedina · Jon Tegnér
Defence Security Systems and Technology, Swedish Defence Research Agency – FOI, SE–147 25 Tumba, Stockholm, Sweden

of experiments, and the goal of using numerical simulations to analyze actual flight conditions still remains unreached. Large Eddy Simulation (LES) models, [3, 4], have been proposed as a promising alternative, having the potential to provide both qualitative and quantitative information. The aim of this study is to describe an LES model for high–speed combustion, validate it against experimental data, [5, 6, 7], and use the LES results to describe the underlying physical processes. The goal is to capture the flow physics at a level suitable for analysis, design and optimization of real high–speed flight vehicles, without resolving all of the detail of the flow.

2 LES Model for Supersonic Combustion

The LES model used consists of the balance equations of mass, species mass fractions, momentum and energy, describing advection, diffusion and reactions, [8]. The reactive gaseous mixture is modeled as a linear viscous fluid with Fourier heat conduction and Fickian diffusion, [8]. The viscosity is obtained from Sutherland's law and the thermal conductivity and species diffusivities follow from the viscosity and species (constant) Prandtl and Schmidt numbers, respectively. The mixtures thermal and caloric equations of state are derived under the assumption that each species is a thermally perfect fluid, with tabulated specific heats and formation enthalpies, [8]. The reaction rates are computed from Guldberg–Waage's law of mass action by summation over all participating reactions, with rate constants obtained from modified Arrhenius rate expressions, [10]. The range of scales present in turbulent reacting flows covers about eight orders of magnitude, [4], with the smaller scales being less energetic but important for the chemical kinetics. The LES model employed here is described in more detail in [11], and employs for closure the mixed subgrid flow model, [12], and the Partially Stirred Reactor (PaSR) subgrid turbulence chemistry interaction model, [13]. The LES equations are solved using a fully explicit finite volume scheme, based on the C++ library OpenFoam, [14], utilizing two–stage Runge–Kutta time–integration and monotonicity preserving flux reconstruction algorithms, [15]. The hydrogen (H_2) combustion is modeled by the 5–species 2–step global reaction mechanism of Rogers & Chinitz, [16], and the 8–species and 7–step reduced reaction mechanism of Davidenko et al, [17].

3 Validation and Physics Elucidation

The combustor, [5, 6, 7], consists of a one–sided divergent channel in which a wedge–shaped flameholder is fitted, at the base of which H_2 is injected through a single row of 15 injectors. The combustor has a width of 40 mm, an overall height of 50 mm and a total length of 340 mm, whereas the flameholder is 32 mm long, 6 mm high and located 100 mm downstream of the inlet. Following the work of Oevermann, [2], Fureby, [18] and Genin & Menon, [19], the freestream velocity of the vitiated air is 732 m/s, for a static pressure of 100 kPa and a static temperature of 340 K. The ports for the hydrogen injection system are choked, and the fuel is

assumed to have a velocity of 1200 m/s and static pressure and temperature of 100 kPa and 250 K, respectively.

Two computational configurations are used; the first consist of a narrow domain with three injectors and 6.3 Mcells whereas the second consists of a wide domain with all 15 injectors included and 22.5 Mcells. The grids are topologically similar, and clustered towards the walls, in the wake and around the shear layers. Dirichlet conditions are used for all variables at the inlet and at the H_2–jets at the base of the strut. At the outlet, all variable values are extrapolated from the interior. At the upper, lower, and strut walls, zero Dirichlet conditions are applied to the velocity together with a wall model, [20], whereas zero Neumann conditions are applied to all other variables. All computations are initialized with the state of the incoming air and are continued until the second order statistical moments have converged after about five flow through–times.

Figure 1a shows a perspective view of the combustor with the semi–transparent side–walls and an iso–surface of the vorticity magnitude colored by the temperature, whereas figures 1b and 1c show side views of numerical schlieren images of a non–reacting case with H_2 injection and of a reacting case, respectively. Figure 1a suggests that the reacting flow may be divided into an induction zone, in which turbulence determines the mixing and the progress of combustion, a transitional zone, dominated by coherent structures dynamics, convective mixing and exothermicity, and a turbulent combustion zone dominated by fully developed turbulence, turbulent mixing and lean post combustion. The H_2 jets discharge in the wake of the flameholder, but due to poor convective mixing across the shear layers the cold H_2, the cold air passing trough the combustor and the hot combustion products from downstream do not mix sufficiently until some distance downstream of the wake, where most of the heat release occurs. Unsteady combustion is also observed to take place in the shear layers, shed–off the edges of the flameholder, preventing the flame from blowing out. The vorticity initially consist of spanwise vortices shed off the flameholder but due vortex–stretching, volumetric expansion and interactions with reflected shocks, a less organized vorticity pattern rapidly develops that is dominated by a combination of longitudinal and distorted spanwise vortices. With inert H_2 injection, figure 1b, oblique shocks are formed at the tips of the flameholder that are reflected by the walls before interacting further with the unsteady, partly H_2 filled, wake. Together with the curved expansion fan coming off the base of the flameholder this causes a characteristic shock wave pattern further downstream. At the walls, the boundary layer is affected, at least locally, by the reflected oblique shocks. These local modifications involve thickening of the boundary layer, increased rms–pressure fluctuations, and elevated wall temperatures. With H_2 injection and combustion, figure 1c, the expansion fans at the upper and lower corners of the flameholder essentially vanish, whereas the recompression shocks become weaker as compared to the inert H_2 injection case. With combustion, the recirculation region becomes longer and wider, and serves as a flameholder for the H_2 diffusion flame. Good agreement is obtained between the predicted and experimental shadowgraph images presented in [7].

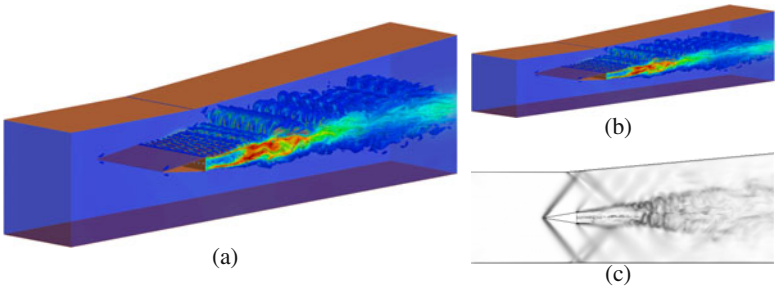

Fig. 1 Flow visualizations in terms of (a) vorticity magnitude colored by temperature and numerical schlieren of (b) non-reacting and (c) reacting case in the wide computational doamin.

In figure 2 we compare predicted and measured time–averaged axial velocity and temperature distributions across the combustor at four cross–sections downstream of the flameholder. Included in this comparison are also earlier LES results using a two–equation flamelet model, [18], with essentially the same laminar flame speed as the 2-step and 7-step reduced mechanisms used in the LES-PaSR simulations. Both the time–averaged axial velocity and temperature show satisfactory agreement with the experimental data for all models investigated, but with the flamelet model performing the least accurate and the 7–step PaSR model performing the most accurate. This suggests that the chemistry by itself is important and that also the resolved turbulence chemistry interactions play a main role in this flow, as can be understood from noticing that the time–scales of the chemistry and the flow are similar. Furthermore, by comparing the 7–step PaSR LES predications in the narrow and wide domains with the experimental data, we find the best overall agreement for the 7–step PaSR LES on the wide domain, in spite of that domain having a coarser grid resolution than the narrow domain. The reason for this is that the spanwise extent of the computational domain must be sufficiently large for spanwise instabilities to develop, and for a sufficient number of longitudinal vortex structures to be maintained in order to support the fully turbulent flow far downstream. In general, all LES presented here tend to underpredict the mean width of the wake at x/h=20.8 and overpredict time–averaged temperatures in the shear layers at x/h=13.0. The agreement between the measured and predicted time–averaged axial velocity profiles at x/h=13.0 is only fair, perhaps due to difficulties in performing accurate measurements in the highly turbulent wake region. Far downstream, at x/h=38.8, only the 7–step PaSR predictions in the narrow and wide domains are able to reproduce the time–averaged temperature, supporting the aforementioned importance of the the chemistry and the resolved turbulence chemistry interactions.

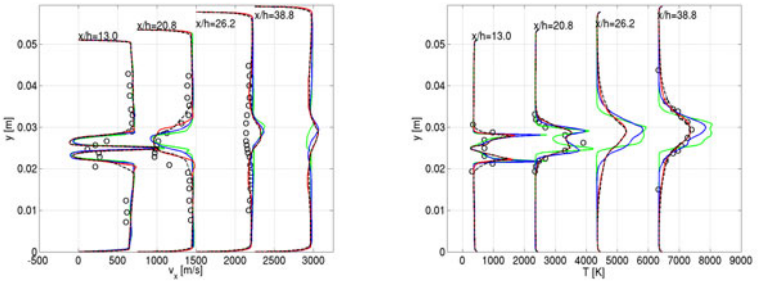

(a) (b)

Fig. 2 Comparison of time averaged (a) axial velocity and (b) temperature profiles across the combustor at four different cross-sections x/h with h being the height of the flameholder. Legend: (○) experimental data, [7], (–) LES using a two–equation flamelet model, [18], (–) LES using a 2–step PaSR model in the narrow domain, (–) LES using a 7–step PaSR model in the narrow domain and (–) LES using a 7–step PaSR model in the wide domain.

4 Summary and Concluding Remarks

In the present work LES has been used to investigate mixing and combustion in a scramjet engine model under realistic operating conditions. Two different LES combustion models have been tested; a flamelet model and a PaSR model, and two different computational domains have been used; a narrow domain with three injectors and a wide domain with 15 injectors. Two different chemical reaction mechanisms have been used together with the LES–PaSR model; a 2–step global mechanism and a 7–step reduced mechanism. Best agreement between experimental data for the time–averaged velocity and temperature is obtained for the 7–step LES PaSR model, with particular good agreement observed in the wide computational domain, due to maintained spanwise development of flow instabilities. The flow physics analysis revealed that most of the heat–release occur downstream of the wake due insufficient mixing across the shear layers. Unsteady (or intermittent) combustion is however observed in the shear layers, thereby essentially preventing the flame from blowing out.

Acknowledgments. The presented work was supported by the Swedish Armed Forces and the Swedish Defense Material Agency and we also acknowledge the DLR Institute of Space Propulsion, Lampoldshausen for providing the experimental data.

References

1. Curran, E., Murthy, S. (eds.): Scramjet Propulsion, ch. 189. AIAA (2000)
2. Oevermann, M.: Aerosp. Sci. Tech. 4, 463 (2000)
3. Ladiende, F. (ed.): Special issue on Scramjet Combustion Technology (2010)
4. Menon, S., Fureby, C.: Computational Combustion. John Wiley & Sons (2010)
5. Oschwald, M., Guerra, R., Waidmann, W.: Int. Symp. on Special topics in Chem. Prop., p. 498 (1993)

6. Waidmann, W., Brummund, U., Nuding, J.: 8th Int. Symp. on Transp. Phenom. in Comb., p. 1473 (1995)
7. Waidmann, W., Alff, F., Brummund, U., Böhm, M., Clauss, W., Oschwald, M.: Space Tech. 15, 421 (1995)
8. Oran, E., Boris, J.: Numerical Simulation of Reactive Flow. Cambridge University Press, Cambridge (2001)
9. Poinsot, T., Veynante, D.: Theoretical and Numerical Combustion. R. T. Edwards, Philadelphia (2001)
10. Levine, R.: Molecular Reaction Dynamics. Cambridge University Press, Cambridge (2005)
11. Berglund, M., Fedina, E., Fureby, C., Tegner, J., Sabel'nikov, V.: AIAA Journal 48, 540 (2010)
12. Bensow, R., Fureby, C.: J. Turb. 8 (2007)
13. Baudoin, E., Nogenmyr, K., Bai, X., Fureby, C.: AIAA 2009-1178 (2009)
14. Weller, H., Tabor, G., Jasak, H., Fureby, C.: Comp. in Physics 12, 629 (1997)
15. Drikakis, D., Hahn, M., Grinstein, F., DeVore, C., Fureby, C., Liefvendahl, M., Youngs, D.: Numerics for ILES: Limiting Algorithms, ch. 4a. Cambridge University Press (2007)
16. Rogers, R., Chinitz, W.: AIAA Journal 21, 586 (1983)
17. Davidenko, D., Gökalp, I., Dufour, E., Marge, P.: 14th AIAA/AHI Space Planes and Hypersonic Systems and Technologies Conference (2006)
18. Berglund, M., Fureby, C.: 31st Int. Symp. on Comb. p. 2491 (2006)
19. Genin, F., Menon, S.: AIAA 2009-0132 (2009)
20. Fureby, C.: Ercoftac Bulletin. Marsh Issue (2007)